Published by Institute of Physics Publishing for SISSA
Received: *May 29, 2008*
Accepted: *July 1, 2008*
Published: *July 21, 2008*

A numerical study of gluon scattering amplitudes in $\mathcal{N} = 4$ super Yang-Mills theory at strong coupling

Suguru Dobashi

Department of Accelerator and Medical Physics,
National Institute of Radiological Sciences,
4-9-1 Anagawa, Inage-ku, Chiba 263-8555, Japan
E-mail: doba@th.phys.titech.ac.jp

Katsushi Ito and Koh Iwasaki

Department of Physics, Tokyo Institute of Technology,
2-12-1, Ookayama, Meguro-ku, Tokyo, 152-8551, Japan
E-mail: ito@th.phys.titech.ac.jp, iwasaki@th.phys.titech.ac.jp

Abstract: We study gluon scattering amplitudes in $\mathcal{N} = 4$ super Yang-Mills theory at strong coupling via the AdS/CFT correspondence. We solve numerically the discretized Euler-Lagrange equations on the square worldsheet for the minimal surface with light-like boundaries in AdS spacetime. We evaluate the area of the surface for the 4, 6 and 8-point amplitudes using worldsheet and radial cut-off regularizations. Their infrared singularities in the cut-off regularization are found to agree with the analytical results near the cusp less than 5% at 520×520 lattice points.

Keywords: Gauge-gravity correspondence, Extended Supersymmetry, AdS-CFT Correspondence.

JHEP07(2008)088

Contents

JHEP07(2008)088

1. Introduction

Recently Alday and Maldacena [1] proposed the prescription for the calculation of gluon scattering amplitudes in $\mathcal{N} = 4$ super Yang-Mills (SYM) theory at strong coupling via the AdS/CFT correspondence. They showed that the gluon scattering amplitude is related to the area of a minimal surface in AdS spacetime surrounded by the Wilson loop with light-like boundaries. They found the exact solution of the minimal surface corresponding to the 4-point amplitude and showed that it reproduces the perturbative formula conjectured by Bern, Dixon and Smirnov (BDS) [2].

The correspondence between gluon amplitudes and the Wilson loops has been examined also at weak coupling [3]. It is shown in [4] that the Wilson loops at weak coupling obey the anomalous conformal Ward identity, which determines the $n = 4$ and 5-point amplitudes completely. For $n \geq 6$-point amplitudes, however, the conformal invariance of the amplitudes does not fix their dependence on the kinematical variables. Recently it is found that the 6-point 2-loop corrections to the Wilson loop agrees numerically with the gluon amplitudes but they differ from the BDS formula [5].

In order to study gluon scattering amplitudes at strong coupling using the AdS/CFT correspondence, we need to find the solution of the minimal surface in AdS spacetime surrounded by the light-like Wilson loop. See [6 – 12, 15] for references. The minimal surface is obtained by solving the Euler-Lagrange equations with the Dirichlet boundary conditions. These are non-linear partial differential equations and highly non-trivial to solve analytically for the polygon with $n \geq 5$ boundaries. Any exact solution for $n \geq 5$ is not yet known so far. In a previous paper [9], the authors including the two authors in the present paper, constructed solutions for the 6 and 8-point amplitudes by cutting and gluing the 4-point amplitude. The evaluation of the amplitudes shows that they do

not agree with the BDS formula both for the infrared singularity and finite parts. In particular, the infrared singularities coincide with those of the 4-point amplitudes, which suggests that these simple solutions are not the minimal surfaces and might correspond to the other disconnected amplitudes.

In this paper we will propose a practical approach to compute the minimal surface in AdS spacetime. We investigate numerically the solution of the Euler-Lagrange equations for the minimal surface in AdS spacetime, surrounded by the light-like segments. We solve the discretized Euler-Lagrange equations on the square lattice with the Dirichlet boundary conditions. We evaluate the area of the surface for the 4, 6 and 8-point amplitudes using two types of cut-off regularizations. One is the world-sheet cut-off regularization. The other is the radial cut-off regularization [13]. For the 4-point amplitude we see that the numerical result agrees with the analytical solution obtained by Alday and Maldacena. For the 6 and 8-point solutions, we take the same momenta configuration as in [9]. The results are different from the cut and glue solutions and there appear new cusp singularities. Their infrared singularities are found to agree with analytical solutions near the cusp. This numerical approach would be a useful method to calculate the n-point gluon amplitudes at strong coupling and test the BDS conjecture from the AdS side.

The paper is organized as follows. In section 2 we describe the discretized Euler-Lagrange equations in AdS spacetime and solve the equations numerically. In section 3, we evaluate the area of the minimal surface for 4, 6 and 8-point amplitudes by using the cut-off regularization in the radial direction of AdS spacetime [13]. We compare their infrared singularity part with the analytical results near the cusp. Section 5 includes conclusions and some comments.

2. The Euler-Lagrange equations of the minimal surface

2.1 Analytical solutions

In this paper we investigate the minimal surface in AdS_5 surrounded by the curve C_n made of light-like segments $\Delta y^\mu = 2\pi p_i^\mu$, which corresponds to the n-point gluon amplitude with on-shell momenta p_i ($p_i^2 = 0$, $i = 1, \ldots, n$). Here y^μ ($\mu = 0, 1, 2, 3$) together with the radial coordinate r are the Poincaré coordinates in AdS_5 spacetime with the metric

$$ds^2 = R^2 \frac{dy^\mu dy_\mu + dr^2}{r^2}, \tag{2.1}$$

and R is the radius of AdS_5. It is convenient to write the Nambu-Goto action in the static gauge where we put $y_3 = 0$ and parametrize the surface by y_1 and y_2. Then r and y_0 are functions of y_1 and y_2 and the action is given by

$$S = \frac{R^2}{2\pi} \int dy_1 dy_2 \frac{\sqrt{1 + (\partial_i r)^2 - (\partial_i y_0)^2 - (\partial_1 r \partial_2 y_0 - \partial_2 r \partial_1 y_0)^2}}{r^2}. \tag{2.2}$$

The Euler-Lagrange equations become

$$\partial_i \left(\frac{\partial L}{\partial(\partial_i y_0)} \right) = 0, \quad \partial_i \left(\frac{\partial L}{\partial(\partial_i r)} \right) - \frac{\partial L}{\partial r} = 0, \tag{2.3}$$

where L is the Lagrangian of the action. The minimal surface is obtained by solving the Euler-Lagrange equations (2.3), which are non-linear partial equations and difficult to solve analytically.

For $n = 4$, Alday and Maldacena found the exact solution [1]. Let us consider the scattering amplitude for two incoming particles with momenta p_1 and p_3 and outgoing particles with momenta p_2 and p_4. The Mandelstam variables are given by $s = -(p_1+p_2)^2$ and $t = -(p_2+p_3)^2$. The case with $s = t$ is particularly simple where the Wilson loop is represented by the square with corners at $y_1, y_2 = \pm 1$. The momenta in the (y_0, y_1, y_2)-space associated with the square are

$$2\pi p_1 = (2, 2, 0), \quad 2\pi p_2 = (-2, 0, 2), \quad 2\pi p_3 = (2, -2, 0), \quad 2\pi p_4 = (-2, 0, -2). \tag{2.4}$$

The boundary conditions for the case with $s = t$ are given by

$$r(\pm 1, y_2) = r(y_1, \pm 1) = 0, \quad y_0(\pm 1, y_2) = \pm y_2, \quad y_0(y_1, \pm 1) = \pm y_1. \tag{2.5}$$

The solution of the Euler-Lagrange equations satisfying the boundary conditions is

$$y_0(y_1, y_2) = y_1 y_2, \quad r(y_1, y_2) = \sqrt{(1 - y_1^2)(1 - y_2^2)}. \tag{2.6}$$

By applying the conformal transformation $\mathrm{SO}(2, 4)$ one can obtain the solution with general s and t. Using the dimensional regularization, the area is shown to agree with the BDS formula at strong coupling.

Noticing that the solution (2.6) satisfies eq. (2.3) even when we change the sign of y_0, an obvious and simple generalization of this remarkable 4-point solution is to cut and glue the solution. In [9], we have constructed 6-point and 8-point solutions of the same action. These cut and glue solutions are summarized as follows:

6-point function solution 1.

$$y_0 = \frac{1}{2}(|y_1 y_2| + y_1 y_2 - |y_1|y_2 + y_1|y_2|), \quad r = \sqrt{(1 - y_1^2)(1 - y_2^2)}. \tag{2.7}$$

The solution corresponds to the scattering with momenta

$$\begin{aligned} &2\pi p_1 = (2, 0, -2), && 2\pi p_2 = (-1, 1, 0), && 2\pi p_3 = (1, 1, 0), \\ &2\pi p_4 = (-1, 0, 1), && 2\pi p_5 = (1, 0, 1), && 2\pi p_6 = (-2, -2, 0). \end{aligned} \tag{2.8}$$

6-point function solution 2.

$$y_0 = y_1|y_2|, \quad r = \sqrt{(1 - y_1^2)(1 - y_2^2)}. \tag{2.9}$$

The momenta are

$$\begin{aligned} &2\pi p_1 = (1, 0, -1), && 2\pi p_2 = (-1, 0, -1), && 2\pi p_3 = (2, 2, 0), \\ &2\pi p_4 = (-1, 0, 1), && 2\pi p_5 = (1, 0, 1), && 2\pi p_6 = (-2, -2, 0). \end{aligned} \tag{2.10}$$

8-point function.

$$y_0 = |y_1 y_2|, \quad r = \sqrt{(1-y_1^2)(1-y_2^2)}. \tag{2.11}$$

The momenta are

$$\begin{aligned} &2\pi p_1 = (-1,0,-1), && 2\pi p_2 = (1,0,-1), && 2\pi p_3 = (-1,1,0), \\ &2\pi p_4 = (1,1,0), && 2\pi p_5 = (-1,0,1), && 2\pi p_6 = (1,0,1), \\ &2\pi p_7 = (-1,-1,0), && 2\pi p_8 = (1,-1,0). \end{aligned} \tag{2.12}$$

These solutions do not reproduce the BDS formula. The most significant discrepancy appears in their infrared singularities. In fact, these solutions have the same infrared divergences as the 4-point amplitude. These solutions have also the delta function source term in the equation of motion. It has been discussed in [9] that these are not the minimal surface and correspond to other disconnected diagrams in field theory.

The main purpose of this paper is to explore numerically the minimal surface corresponding to the same boundary conditions as the above higher-point solutions. In this paper we will study the square worldsheet for simplicity. We will make a comment on a generalization to the light-like hexagon Wilson loop in section 4.

2.2 Discretized Euler-Lagrange equations

We firstly introduce the square lattice with spacing $h = \frac{2}{M}$ where M is a positive integer. At each site $(-1+hi, -1+hj)$ $(i,j = 0,\ldots,M)$, we assign the variables

$$y_0[i,j] = y_0(-1+hi,-1+hj), \quad r[i,j] = r(-1+hi,-1+hj). \tag{2.13}$$

We use the central difference method to discretize the Euler-Lagrange equations. Namely, for a function $f(y_1,y_2)$ we adopt the following rules to obtain the difference equations from the differential equations:

$$\begin{aligned} \partial_1 f(y_1,y_2) &\longrightarrow \frac{f[i+1,j]-f[i-1,j]}{2h}, \\ \partial_2 f(y_1,y_2) &\longrightarrow \frac{f[i,j+1]-f[i,j-1]}{2h}, \\ \partial_1\partial_2 f(y_1,y_2) &\longrightarrow \frac{f[i+1,j+1]-f[i+1,j-1]-f[i-1,j+1]+f[i-1,j-1]}{4h^2}, \\ \partial_1^2 f(y_1,y_2) &\longrightarrow \frac{f[i+1,j]-2f[i,j]+f[i-1,j]}{h^2}, \\ \partial_2^2 f(y_1,y_2) &\longrightarrow \frac{f[i,j+1]-2f[i,j]+f[i,j-1]}{h^2}. \end{aligned} \tag{2.14}$$

We need to specify the boundary conditions to solve the equations. For example, the boundary conditions (2.5) for the 4-point solutions lead to

$$\begin{aligned} &y_0[i,0] = y_0(-1+hi,-1), && y_0[i,M] = y_0(-1+hi,1), \\ &y_0[0,j] = y_0(-1,-1+hj), && y_0[M,j] = y_0(1,-1+hj), \\ &r[i,0] = r[i,M] = r[0,j] = r[M,j] = 0. \end{aligned} \tag{2.15}$$

JHEP07(2008)088

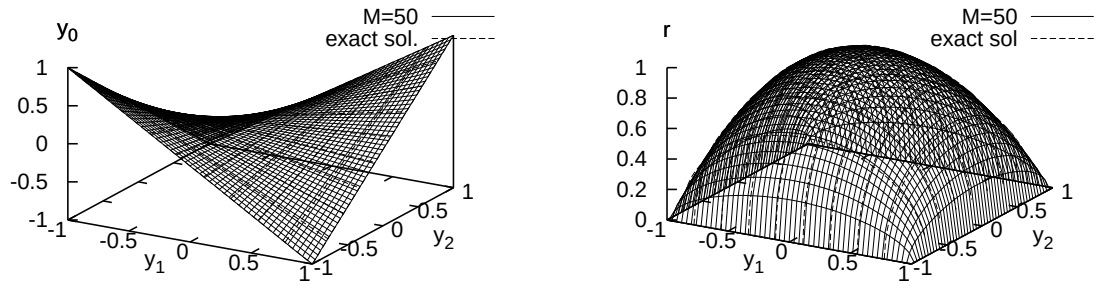

(a) (b)

Figure 1: Numerical solution of the 4-point amplitude at $M = 50$.

Then we obtain $2 \times (M-1)^2$ nonlinear simultaneous equations for $y_0[i,j]$ and $r[i,j]$. We will use Newton's method to find a numerical solution. In this method the initial solution is important to get good numerical results iteratively. The approximate solution will soon converge if the initial numerical data is appropriate. Otherwise, the numerical solution does not converge and the surface would not be smooth. We take as the initial condition the Alday-Maldacena solution for 4-point function or cut and glue solutions for 6 and 8-point functions. But some trials show that the cut and glue solution does not lead to convergence when the lattice size becomes large. So we begin with the $M = 10$ lattice with these initial conditions and proceed step by step to larger size of lattices, up to $M = 520$,[1] with the output of a previous smaller lattice calculation being the input for the next larger lattice, by linearly interpolating the output. For each lattice size, the Newton's method is repeatedly applied until the non-linear simultaneous equation is satisfied up to $\mathcal{O}(10^{-16})$ and the area of the obtained surface does not change up to $\mathcal{O}(10^{-6})$ even when we proceed to the next step of the Newton's method. The area is approximately evaluated as $S = \sum L[i,j]h^2$, where $L[i,j]$ and h are the discretized Lagrangian at a lattice point (i,j) and the lattice spacing, respectively.

We plot numerical solutions at $M = 50$ in figure 1, where we can see the 4-point solution apparently agrees with the exact solution. This agreement with the exact solution is quantitatively checked by comparing the areas between numerical and exact solutions in the next section. In figures 2, 3 and 4, we plot numerical solutions of the 6-point and 8-point amplitudes with the same boundary conditions as the cut and glue solutions. We find that the numerical solutions are different from the cut and glue solutions and new cusps seem to appear which are absent in the cut and glue solutions [9]. In the next section we will evaluate the area of the surface numerically and examine the infrared behavior of the regularized area.

[1] A numerical computation was carried out by Mathematica and C programs on a personal computer with 8GB memory, which restricts the lattice size to $M = 520$.

JHEP07(2008)088

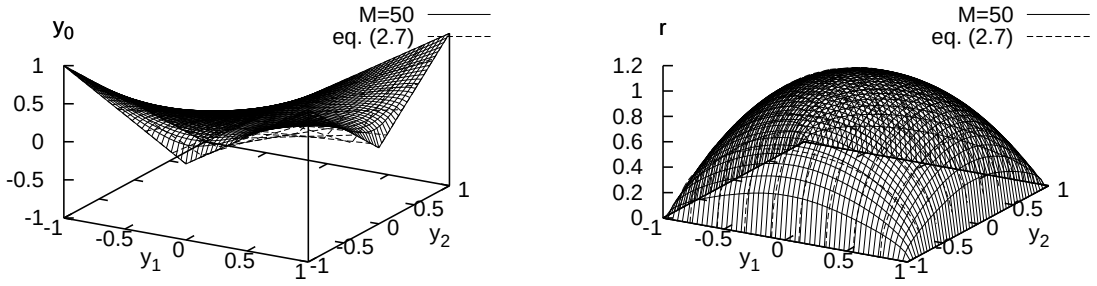

(a) (b)

Figure 2: Numerical solution of 6-point amplitude solution 1 (a) y_0 (b) r at $M = 50$.

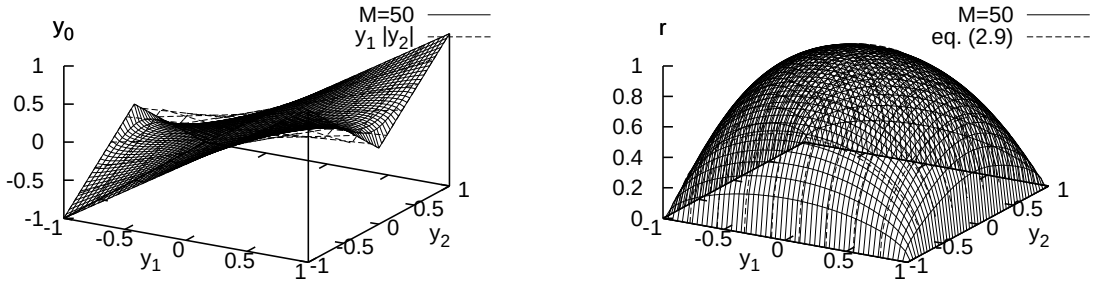

(a) (b)

Figure 3: Numerical solution of 6-point amplitude solution 2 (a) y_0 (b) r at $M = 50$.

3. The cut-off regularization and the minimal area

In order to study the gluon scattering amplitude, we need to evaluate the area of the minimal surface in AdS spacetime. Since we have obtained numerically the solution of the surface from the discretized Euler-Lagrange equations, we can evaluate it easily. But for a light-like Wilson loop, the value of the area diverges due to the cusp [14, 1]. We often use the dimensional regularization scheme to control this divergence, which is convenient to compare the area with the field theory result. But in order to calculate the area numerically in the present discretization procedure, it is better to use cut-off regularization. In a recent paper [13], a cut-off r_c in the radial coordinate is introduced to regularize the action, which characterizes the cusp divergences in a simple way. In this section, we will compare our numerical results with the cut-off formula and see that our results numerically agree with the cut-off regularized formula of the n-point amplitudes.

JHEP07(2008)088

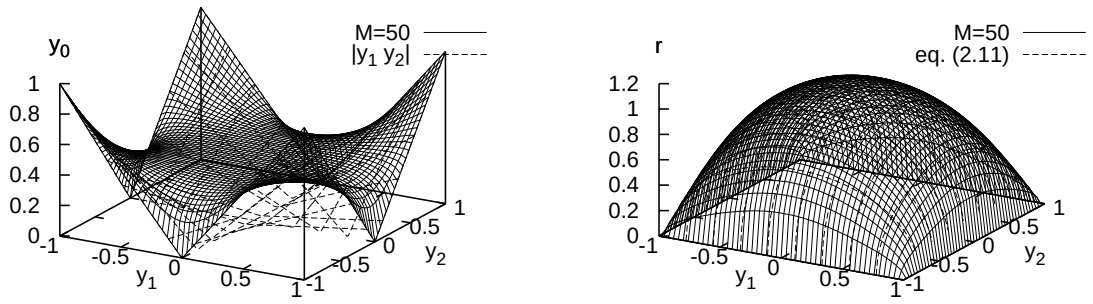

(a) (b)

Figure 4: Numerical solution of 8-point amplitude (a) y_0 (b) r at $M = 50$.

3.1 The worldsheet cut-off regularization

Before going to the radial cut-off formula, we will consider a simple worldsheet cut-off regularization, where we restrict the integration region of (y_1, y_2) in the action (2.2) to $[-1+\delta, 1-\delta] \times [-1+\delta, 1-\delta]$ for small δ. Substituting the 4-point solution (2.6) into the Lagrangian L, we get

$$L = \frac{1}{(1-y_1^2)(1-y_2^2)}. \tag{3.1}$$

Here we omit the overall factor $\frac{R^2}{2\pi}$ in the action. Then the regularized action $S[\delta]$ is defined by

$$S[\delta] = \int_{-1+\delta}^{1-\delta} dy_1 dy_2 \frac{1}{(1-y_1^2)(1-y_2^2)}. \tag{3.2}$$

This integral is evaluated easily and we obtain

$$S[\delta] = \left(\log \frac{2-\delta}{\delta}\right)^2. \tag{3.3}$$

The infrared singularity around the cusp appears as the $(\log \delta)^2$ divergence, which corresponds to the double pole $\frac{1}{\epsilon^2}$ in the dimensional regularization scheme.

We have seen that $S[\delta]$ for cut and glue solutions of 6 and 8-points amplitudes is the same as the 4-point amplitude [9]. In figure 5, we plot the $\delta - S[\delta]$ graph for 4, 6, and 8-point functions. From the graphs we see that there exist differences among the regularized actions, especially near the boundaries (i.e. small δ). This fact indicates that our numerical 6 and 8-point solutions have different divergent properties from cut and glue solutions. We see differences between numerical and exact results for the 4-point amplitude at small δ region. These are due to the fact that the numerical results are quite sensitive with the errors which come from the discretization of r near the boundary. However, the discrepancy at a given δ is suppressed when the lattice size increases, as we will see later.

Since we do not know exact functional form of new numerical solutions, the δ-dependence of the numerical $S[\delta]$ for higher-point amplitudes is not clear. Roughly we

JHEP07(2008)088

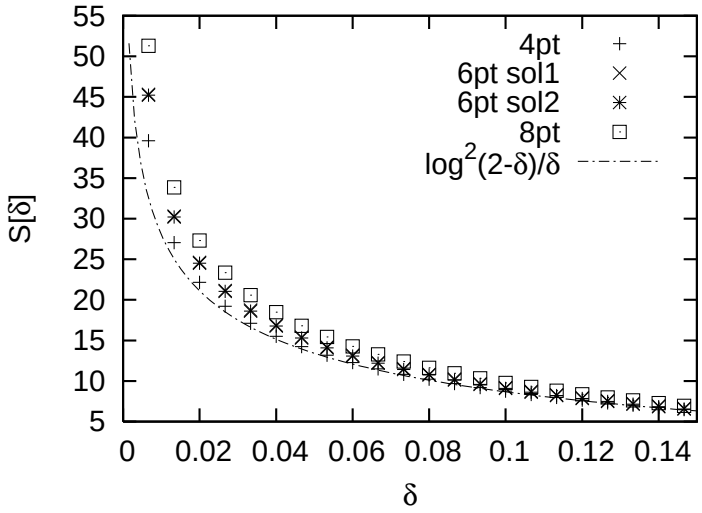

Figure 5: $\delta - S[\delta]$ graphs at $M = 300$.

	a	b	c
4-point	1.12352	-1.16767	0.101811
6-point sol. 1	1.40647	-0.648713	0.214939
6-point sol. 2	1.41405	-0.58385	0.241626
8-point	1.67364	-0.26576	0.280678

Table 1: Fitting parameters of $M = 300$ data using (3.4).

can identify $\log \delta$ as $\frac{1}{\epsilon}$. It would not be a bad approximation to use a fitting function:

$$a(\log \delta)^2 + b(\log \delta) + c, \tag{3.4}$$

for $S[\delta]$. Table 1 is a list of the value of a, b and c for each data fitted in the region $0.04 < \delta < 1.14$. The leading singularities are different for 4, 6 and 8 point amplitudes. But for solution 1 and solution 2 of 6-point functions they agree: $a_{4\text{pt}} < a_{6\text{ptsol1}} \sim a_{6\text{ptsol2}} < a_{8\text{pt}}$. This is consistent with the expected infrared leading singularity behaviour $const. \times n(\log \delta)^2$ for the n-point amplitude [2].

It is a hard problem to estimate rigorously numerical errors in our approximation. But in the case of the 4-point amplitude, for which the exact solution has been obtained, we can see several positive features which support the validity of our numerical approach. Figure 6 shows the behaviour of the numerical solution for r on the $y_2 = 0$ plane near the boundary. We can see that the numerical solution approaches the exact one as M increases. Although we omit further details, it can be also shown that the solution is not affected by smooth and small modification of the initial condition. In addition, the area of the surface approaches to the exact result as M becomes larger and larger. In table 2 and figure 7, we exhibit the behaviours of the cut-off regularized area for $\delta = 0.1$ and $\delta = 0.2$,

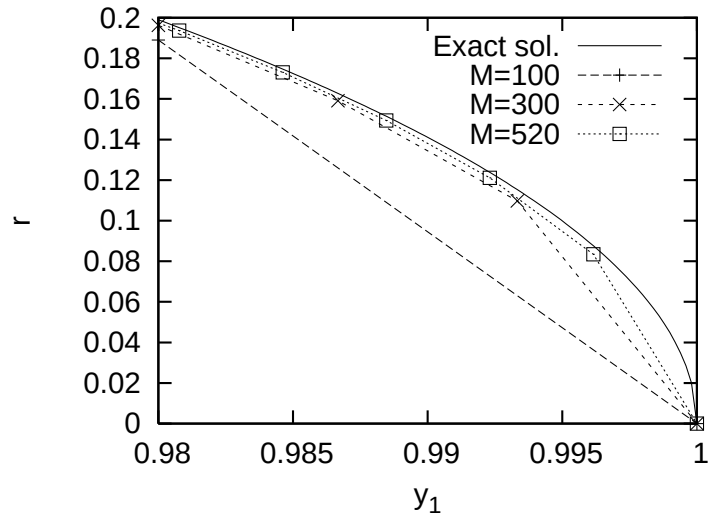

Figure 6: Near boundary behavior of r on $y_2 = 0$ plane for several M's (4-point solution).

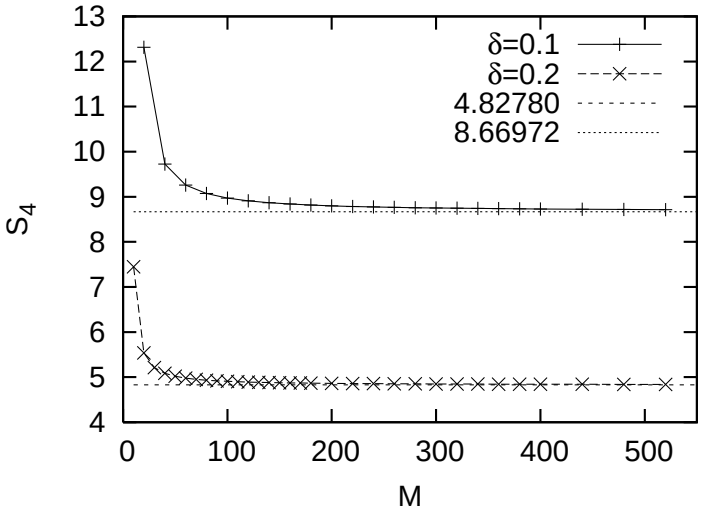

Figure 7: Regularized area at $\delta = 0.1$ and $\delta = 0.2$ for several M's (4-point solution).

which shows good convergence to the analytical results, with the error being about 0.2% for the $\delta = 0.2$, $M = 520$ case.

This artificial worldsheet cut-off is not invariant under conformal transformation of the worldsheet. This regularization heavily depends on the static gauge. In order to regularize the action in a conformal invariant way, it is better to introduce the radial cut-off as in [13].

3.2 The radial cut-off regularization

In the radial cut-off regularization scheme we introduce a cut-off r_c in the radial direction [13]. The regularized area is surrounded by the cut-off curve $C : r_c = r(y_1, y_2)$. For

JHEP07(2008)088

M	S_4	$(S_4 - S_e)/S_e$
100	8.97215	0.03488390
200	8.80018	0.01504770
300	8.75113	0.00939031
520	8.71324	0.00501923

(a) $\delta = 0.1$

M	S_4	$(S_4 - S_e)/S_e$
100	4.90702	0.01641050
200	4.86233	0.00715303
300	4.84934	0.00446242
520	4.83927	0.00237603

(b) $\delta = 0.2$

Table 2: Convergent behavior of cut-off regularized area for the 4-point solution. S_4 and S_e are numerical and exact results, respectively.

example, the curve of the 4-point amplitude with $s = t$ is

$$r_c^2 = \left(1 - y_1^2\right)\left(1 - y_2^2\right). \tag{3.5}$$

The regularized action is the area of the region S whose boundary is C:

$$\tilde{S}[r_c] = \int_S dy_1 dy_2 \frac{1}{(1-y_1^2)(1-y_2^2)}. \tag{3.6}$$

For fixed y_1, the integration region of y_2 is $-y_2^c \le y_2 \le y_2^c$, where $y_2^c (> 0)$ is given by

$$(y_2^c)^2 = 1 - \frac{r_c^2}{1-y_1^2}. \tag{3.7}$$

After the integration over y_2, we get

$$\tilde{S}[r_c] = \int_{-\sqrt{1-r_c^2}}^{\sqrt{1-r_c^2}} dy_1 \frac{1}{1-y_1^2} \log\left(\frac{\sqrt{1-y_1^2} + \sqrt{1-r_c^2-y_1^2}}{\sqrt{1-y_1^2} - \sqrt{1-r_c^2-y_1^2}}\right). \tag{3.8}$$

Since we are interested in the small r_c limit, we expand the integrand $f(y_1, r_c)$ in r_c:

$$f(y_1, r_c) = -\frac{2\log r_c - \log(4-4y_1^2)}{1-y_1^2} + \frac{r_c^2}{2(1-y_1^2)} + \cdots. \tag{3.9}$$

The integral over y_1 leads to

$$\tilde{S}[r_c] = \frac{1}{2}\left(\log\frac{r_c^2}{16}\right)^2 - 2(\log 2)^2 - \frac{\pi^2}{16} + O(r_c^2). \tag{3.10}$$

The general (s,t) solution has been found in [1], which can be obtained by scale and boost transformation of the $s = t$ solution:

$$r' = \frac{ar}{1+by_0}, \quad y_0' = \frac{a\sqrt{1+b^2}y_0}{1+by_0}, \quad y_i' = \frac{ay_i}{1+by_0}, \tag{3.11}$$

where a is a parameter for the scale transformation and b the boost parameter. The Mandelstam variables s and t are given by

$$(2\pi)^2 s = -\frac{8a^2}{(1-b)^2}, \quad (2\pi)^2 t = -\frac{8a^2}{(1+b)^2}. \tag{3.12}$$

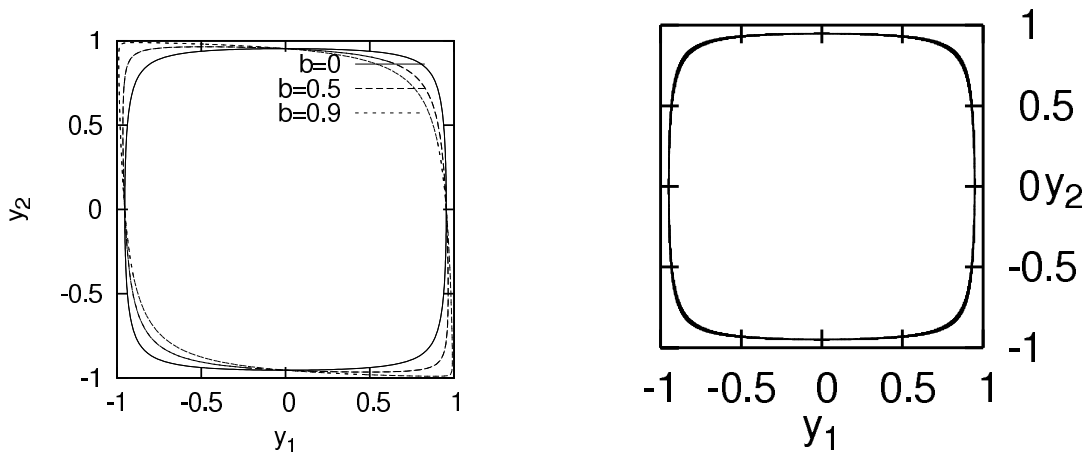

(a) (b)

Figure 8: (a)The cut-off curves with $\frac{r_c}{a} = 0.3$ and $b = 0, 0.5, 0.9$ (b) The cut-off curve with $\frac{r_c}{a} = 0.3$ from the numerical data (4-point solution $M = 300$).

The cut-off curve (3.5) (see figure 8 (a)) is now replaced by

$$r_c^2 = a^2(1-y_1^2)(1-y_2^2)\frac{1}{(1+by_1y_2)^2}. \tag{3.13}$$

We can put $a = 1$ by rescaling $r_c \to r_c a$. For fixed y_1, y_2 takes the value in the range $y_2^{c-} \le y_2 \le y_2^{c+}$, where

$$y_2^{c\pm} = \frac{-br_c^2 y_1 \pm \sqrt{(1-y_1^2)(1-y_1^2-r_c^2+b^2r_c^2y_1^2)}}{1-y_1^2+b^2r_c^2y_1^2}. \tag{3.14}$$

The integral over y_2 yields

$$\tilde{S}[r_c] = \int_{-\sqrt{\frac{1-r_c^2}{1-b^2r_c^2}}}^{\sqrt{\frac{1-r_c^2}{1-b^2r_c^2}}} dy_1 f(y_1, r_c), \tag{3.15}$$

where

$$f(y_1, r_c) = \frac{1}{1-y_1^2}\frac{1}{2}\log\left(\frac{1+y_2^{c+}}{1-y_2^{c+}}\frac{1-y_2^{c-}}{1+y_2^{c-}}\right). \tag{3.16}$$

Expanding in r_c we get

$$f(y_1, r_c) = -\frac{1}{1-y_1^2}\log\left(r_c^2\frac{1-b^2y_1^2}{4(1-y_1^2)}\right) + O(r_c^2). \tag{3.17}$$

After the integral over y_1, we get

$$\tilde{S}[r_c] = \frac{1}{4}\log^2\left(\frac{r_c^2}{-8\pi^2 s}\right) + \frac{1}{4}\log^2\left(\frac{r_c^2}{-8\pi^2 t}\right) - \frac{1}{4}\log^2\left(\frac{s}{t}\right) - 2(\log 2)^2 - \frac{\pi^2}{16} + O(r_c^2). \tag{3.18}$$

This formula of the 4-point amplitude was obtained in [13] using the conformal gauge.

The above analysis for the regularized action of the 4-point amplitude is generalized to examine the infrared singular part of the n-point amplitude, which was done in the dimensional regularization [6]. The infrared singularity of the n-point amplitude is characterized by the cusp made of two external gluon lines with momenta p_i and p_{i+1}. It is convenient to use the light-cone coordinates $y^{\pm} = y^0 \pm y^1$ and regard y_2 and r as the functions of $y^{\pm}$. The Nambu-Goto action in this gauge is

$$S = \frac{R^2}{2\pi}\int dy_- dy_+ \frac{1}{2r^2}\sqrt{1 - 4\partial_- y_2 \partial_+ y_2 - 4\partial_- r\partial_+ r - 4(\partial_- y_2\partial_+ r - \partial_- r\partial_+ y_2)^2}. \quad (3.19)$$

The momenta of the external gluon lines in the (y_-, y_+, y_2) coordinates are parametrized as $2\pi p_i = z_1(0,1,0)$ and $2\pi p_{i+1} = z_2(\alpha, 1, \sqrt{\alpha})$. The Mandelstam variable is $(2\pi)^2 s_{i,i+1} = z_1 z_2(-\alpha) = -z_1 z_2 \alpha$. Then the solution of the equation of motion, which approaches to the cusp solution in the limit $\alpha \to 0$, is

$$r(y_-, y_+) = \sqrt{2}\sqrt{y_-\left(y_+ - \frac{1}{\alpha}y_-\right)}, \quad y_2(y_-, y_+) = \frac{1}{\sqrt{\alpha}}y_-. \quad (3.20)$$

Parameterizing the solution as

$$y_- = \alpha z_2 Y_-, \quad y_+ = z_1 Y_+ + z_2 Y_-, \quad (3.21)$$

we find

$$r(Y_-, Y_+) = \sqrt{2}\sqrt{Y_- Y_+}\sqrt{-(2\pi)^2 s_{i,i+1}}, \quad (3.22)$$

and the action near the cusp is

$$S_{i,i+1} = \frac{R^2}{4\pi}\int_0^1 \frac{dY_- dY_+}{2Y_- Y_+}. \quad (3.23)$$

The action is divergent at the cusp $Y_- = Y_+ = 0$. Introducing the radial cut-off r_c by

$$r_c = \sqrt{2}\sqrt{-(2\pi)^2 s_{i,i+1}}\sqrt{Y_- Y_+}, \quad (3.24)$$

the regularized action rescaled by the factor of $\frac{R^2}{2\pi}$ becomes

$$\begin{aligned}\tilde{S}_{i,i+1} &= \frac{1}{2}\int_{\frac{r_c^2}{A^2}}^1 dY_+ \int_{\frac{r_c^2}{A^2 Y_+}}^1 \frac{1}{2Y_- Y_+} \\ &= \frac{1}{8}\left(\log\frac{r_c^2}{-2(2\pi)^2 s_{i,i+1}}\right)^2. \end{aligned} \quad (3.25)$$

Here $A = \sqrt{2}\sqrt{-(2\pi)^2 s_{i,i+1}}$.

Then the n-point amplitude is expected to have the structure

$$\tilde{S}_n[r_c] = \frac{1}{8}\sum_{i=1}^{n}\left(\log\frac{r_c^2}{-8\pi^2 s_{i,i+1}}\right)^2 + F_n(p_1, \ldots, p_n) + O(r_c^2), \quad (3.26)$$

where $s_{i,i+1} = -(p_i + p_{i+1})^2$ and $p_{n+1} = p_1$. $F_n(p_1, \ldots, p_n)$ is a finite remainder part. The 4-point function with the momenta (2.4) with $s = t$, we obtain $(2\pi)^2 s_{1,2} = -8$. The action is of the form

$$\tilde{S}_4[r_c] = \frac{a_0}{2}\left(\log\frac{r_c^2}{16}\right)^2 + c_0, \tag{3.27}$$

up to $O(r_c^2)$ terms, where $a_0 = 1$ and c_0 is a constant.

For the 6-point function (solution 1 and 2) and the 8-point solution, the amplitudes in the radial cut-off scheme are

$$\tilde{S}_6^1[r_c] = \frac{a_1}{8}\left(4\left(\log\frac{r_c^2}{8}\right)^2 + \left(\log\frac{r_c^2}{4}\right)^2 + \left(\log\frac{r_c^2}{16}\right)^2\right) + c_1, \tag{3.28}$$

$$\tilde{S}_6^2[r_c] = \frac{3}{4}a_2\left(\log\frac{r_c^2}{8}\right)^2 + c_2, \tag{3.29}$$

$$\tilde{S}_8[r_c] = \frac{1}{2}a_3\left(\left(\log\frac{r_c^2}{8}\right)^2 + \left(\log\frac{r_c^2}{4}\right)^2\right) + c_3, \tag{3.30}$$

up to $O(r_c^2)$ terms, where $a_1 = a_2 = a_3 = 1$ and c_1, c_2 and c_3 are constants.

We approximate the area by summing the value of discretized Lagrangian at the lattice points (i, j) at which the value of $r[i, j]$ is larger than the radial cut-off r_c. In figure 9 we show the fitting data of the r_c regularization. The numerical results are fitted to the trial functions with the least-square method in the range $0.15 \leq r_c \leq 3.0$. The lower limit of the fitting range cannot be so small because of the rapid growth of r near the boundary (see figure 6). We reasonably chosen the lower limit as $r_c = 0.15$ so that the lattice points around the boundary which satisfy $r[i, j] > r_c$ are several points inner from the boundary. The approximation error for the area is roughly estimated as the difference between the area estimated above and the one for the nearest outer lattice points. Figure 10 is the result with such errors for the 4-point solutions. We fit the results $S[r_c]$ for each solution with the weight of errors estimated in this way by using 'fit' command of GNUPLOT.

Fitting these data in the region $0.15 \leq r_c \leq 0.3$ by the functions (3.27), (3.28), (3.29) and (3.30) respectively, we find that

$$a_0 = 1.01694, \qquad c_0 = -3.5912, \tag{3.31}$$

$$a_1 = 1.03715, \qquad c_1 = -3.68904, \tag{3.32}$$

$$a_2 = 1.0376, \qquad c_2 = -3.70123, \tag{3.33}$$

$$a_3 = 1.04973, \qquad c_3 = -3.70072. \tag{3.34}$$

We see that our numerical results a_i are in agreement with the radial cut-off regularization formula within a few per cent. The constant c_0 of the 4-point amplitude differs from the cut-off formula (3.10). Therefore we need to take into account for the finite r_c^2 corrections to the area in order to get the finite remainder part. This subject is beyond the scope of the present paper and is left to a future problem.

JHEP07(2008)088

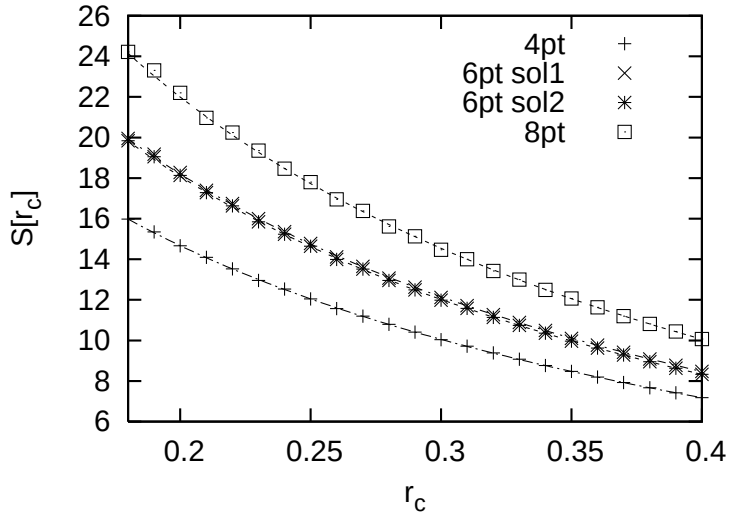

Figure 9: r_c - $\tilde{S}[r_c]$ graph at $M = 520$.

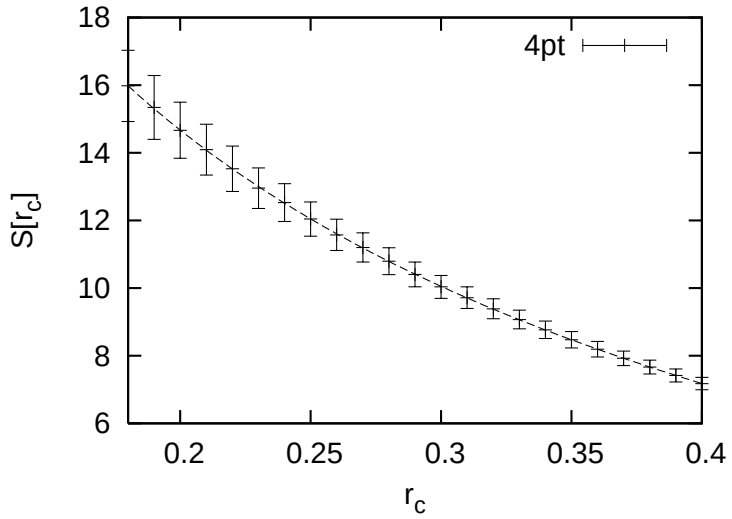

Figure 10: r_c - $\tilde{S}[r_c]$ graph at $M = 520$ with error-bars.

4. Conclusions and discussion

In this paper we have investigated the discretized Euler equations of the minimal surface in AdS spacetime numerically. We examined the minimal surface corresponding to the 4, 6 and 8-point amplitudes, in which the $n \geq 6$ solutions have the same boundary conditions as in [9]. These boundary conditions are simple because the worldsheet in the static gauge is square, which are easy to write a program to solve the system of nonlinear simultaneous equations. Since the area is divergent around the cusps, we have introduced the worldsheet cut-off and radial cut-off regularizations. In the worldsheet cut-off regularization, the 4-

JHEP07(2008)088

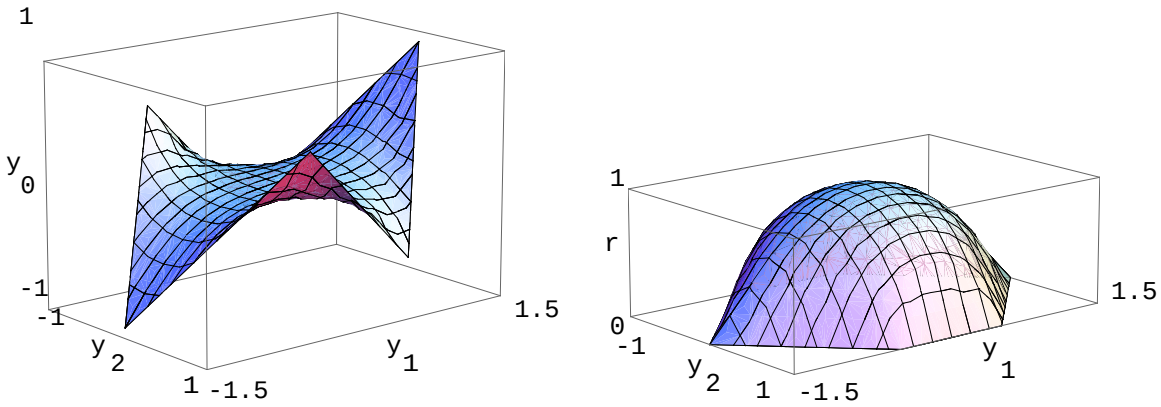

Figure 11: Numerical solution of 6-point function with hexagon boundary (116 lattice points) (a) $y_0(y_1, y_2)$, (b) $r(y_1, y_2)$.

point amplitude agrees numerically with the exact solution within 0.2% for the $\delta = 0.2$, $M = 520$ case. For the radial cut-off regularized amplitudes, we have checked that the infrared singularity part of the area numerically agrees with the analytical result near the cusp within 5% for 520×520 lattice points.

Using conformal transformation of the solution, we are able to study non-trivial momentum dependence of the amplitude including not only the infrared singularity but also the finite part. It is an interesting problem to extract numerically the finite remainder part of the gluon amplitudes from the minimal surface.

One can also generalize the present square worldsheet to polygons. Here we will show an preliminary example of the minimal surface solution with the hexagonal boundary (figure 11), whose momenta are

$$\begin{aligned} &2\pi p_1 = (\sqrt{2}, 1, -1), && 2\pi p_2 = (-\sqrt{2}, -1, -1), && 2\pi p_3 = (1, -1, 0), \\ &2\pi p_4 = (-\sqrt{2}, -1, 1), && 2\pi p_5 = (\sqrt{2}, 1, 1), && 2\pi p_6 = (-1, 1, 0). \end{aligned} \tag{4.1}$$

Here we can see six cusps. The evaluation of the regularized action with polygon lightlike boundary condition gives another nontrivial test of the gluon amplitudes/Wilson loop duality at strong coupling.

Another interesting application of this formalism is the gluon scattering in non-AdS geometry, which is rather difficult to obtain the analytic solution of the Euler-Lagrange equations [11]. A numerical approach will help us to understand their properties at strong coupling. A detailed study of these problems will be discussed elsewhere.

Acknowledgments

K. Ito is supported in part by Ministry of Education, Culture, Sports, Science and Technology of Japan. K. Iwasaki acknowledges support from the Iwanami Fujukai Foundation.

A part of numerical calculations were performed on Sushiki at YITP, Kyoto University and the workstation at theory group, University of Tokyo, Komaba.

References

[1] L.F. Alday and J.M. Maldacena, *Gluon scattering amplitudes at strong coupling*, *JHEP* **06** (2007) 064 [arXiv:0705.0303].

[2] Z. Bern, L.J. Dixon and V.A. Smirnov, *Iteration of planar amplitudes in maximally supersymmetric Yang-Mills theory at three loops and beyond*, *Phys. Rev.* **D 72** (2005) 085001 [hep-th/0505205].

[3] J.M. Drummond, G.P. Korchemsky and E. Sokatchev, *Conformal properties of four-gluon planar amplitudes and Wilson loops*, *Nucl. Phys.* **B 795** (2008) 385 [arXiv:0707.0243];
A. Brandhuber, P. Heslop and G. Travaglini, *MHV amplitudes in $N = 4$ super Yang-Mills and Wilson loops*, *Nucl. Phys.* **B 794** (2008) 231 [arXiv:0707.1153];
J.M. Drummond, J. Henn, G.P. Korchemsky and E. Sokatchev, *On planar gluon amplitudes/Wilson loops duality*, *Nucl. Phys.* **B 795** (2008) 52 [arXiv:0709.2368].

[4] J.M. Drummond, J. Henn, G.P. Korchemsky and E. Sokatchev, *Conformal Ward identities for Wilson loops and a test of the duality with gluon amplitudes*, arXiv:0712.1223.

[5] J.M. Drummond, J. Henn, G.P. Korchemsky and E. Sokatchev, *Hexagon Wilson loop = six-gluon MHV amplitude*, arXiv:0803.1466;
Z. Bern et al., *The two-loop six-gluon MHV amplitude in maximally supersymmetric Yang-Mills theory*, arXiv:0803.1465.

[6] E.I. Buchbinder, *Infrared limit of gluon amplitudes at strong coupling*, *Phys. Lett.* **B 654** (2007) 46 [arXiv:0706.2015].

[7] A. Mironov, A. Morozov and T.N. Tomaras, *On n-point amplitudes in $N = 4$ SYM*, *JHEP* **11** (2007) 021 [arXiv:0708.1625]; *Some properties of the Alday-Maldacena minimum*, *Phys. Lett.* **B 659** (2008) 723 [arXiv:0711.0192];
H. Itoyama, A. Mironov and A. Morozov, *Boundary ring: a way to construct approximate NG solutions with polygon boundary conditions: I. Z_n-symmetric configurations*, arXiv:0712.0159;
H. Itoyama and A. Morozov, *Boundary ring or a way to construct approximate NG solutions with polygon boundary conditions. II. Polygons which admit an inscribed circle*, arXiv:0712.2316;
H. Itoyama, A. Mironov and A. Morozov, *'Anomaly' in $N = \infty$ Alday-Maldacena duality for wavy circle*, *JHEP* **07** (2008) 024 [arXiv:0803.1547].

[8] L.F. Alday and J.M. Maldacena, *Comments on operators with large spin*, *JHEP* **11** (2007) 019 [arXiv:0708.0672].

[9] D. Astefanesei, S. Dobashi, K. Ito and H. Nastase, *Comments on gluon 6-point scattering amplitudes in $N = 4$ SYM at strong coupling*, *JHEP* **12** (2007) 077 [arXiv:0710.1684].

[10] Z. Komargodski and S.S. Razamat, *Planar quark scattering at strong coupling and universality*, *JHEP* **01** (2008) 044 [arXiv:0707.4367];
J. McGreevy and A. Sever, *Quark scattering amplitudes at strong coupling*, *JHEP* **02** (2008) 015 [arXiv:0710.0393].

JHEP07(2008)088

[11] K. Ito, H. Nastase and K. Iwasaki, *Gluon scattering in $\mathcal{N} = 4$ super Yang-Mills at finite temperature*, arXiv:0711.3532.

[12] Y. Oz, S. Theisen and S. Yankielowicz, *Gluon scattering in deformed $N = 4$ SYM*, *Phys. Lett.* **B 662** (2008) 297 [arXiv:0712.3491].

[13] L.F. Alday, *Lectures on scattering amplitudes via AdS/CFT*, arXiv:0804.0951.

[14] M. Kruczenski, *A note on twist two operators in $N = 4$ SYM and Wilson loops in Minkowski signature*, *JHEP* **12** (2002) 024 [hep-th/0210115].

[15] S. Ryang, *Conformal* SO(2, 4) *transformations of the one-cusp Wilson loop surface*, *Phys. Lett.* **B 659** (2008) 894 [arXiv:0710.1673];
A. Popolitov, *On coincidence of Alday-Maldacena-regularized σ-model and Nambu-Goto areas of minimal surfaces*, *JETP Lett.* **86** (2007) 643 [arXiv:0710.2073];
G. Yang, *Comment on the Alday-Maldacena solution in calculating scattering amplitude via AdS/CFT*, *JHEP* **03** (2008) 010 [arXiv:0711.2828];
A. Jevicki, K. Jin, C. Kalousios and A. Volovich, *Generating AdS string solutions*, *JHEP* **03** (2008) 032 [arXiv:0712.1193];
Z. Komargodski, *On collinear factorization of Wilson loops and MHV amplitudes in $N = 4$ SYM*, *JHEP* **05** (2008) 019 [arXiv:0801.3274];
R.C. Brower, H. Nastase, H.J. Schnitzer and C.-I. Tan, *Implications of multi-Regge limits for the Bern-Dixon-Smirnov conjecture*, arXiv:0801.3891.

JHEP07(2008)088